Article

Cell Reports

Signal-Dependent Recruitment of BRD4 to Cardiomyocyte Super-Enhancers Is Suppressed by a MicroRNA

Graphical Abstract

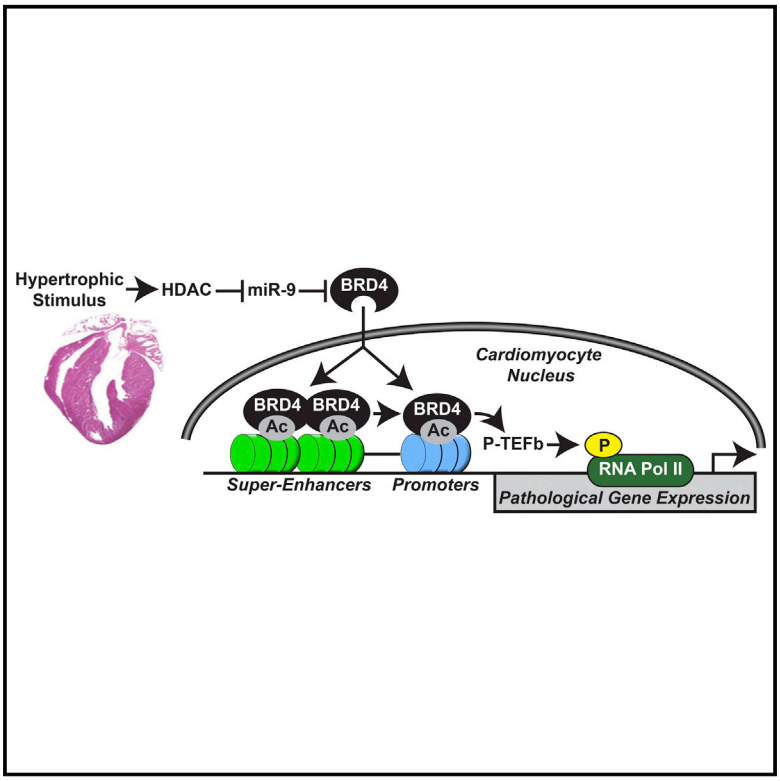

Authors

Matthew S. Stratton, Charles Y. Lin, Priti Anand, ..., James E. Bradner, Saptarsi M. Haldar, Timothy A. McKinsey

Correspondence

timothy.mckinsey@ucdenver.edu

In Brief

Stratton et al. find that downregulation of microRNA-9 leads to derepression of BRD4 and enrichment of BRD4 at long-range super-enhancers associated with pathological cardiac genes. Dynamic enrichment of BRD4 at super-enhancers serves a crucial role in the control of stress-induced cardiac hypertrophy.

Highlights

- Stress stimuli trigger dynamic changes in BRD4 genome targeting in cardiomyocytes
- MicroRNA-9 suppresses BRD4 in cardiomyocytes and restricts cell size
- Downregulation of microRNA-9 is required for recruitment of BRD4 to super-enhancers
- MicroRNA-9 regulates signal-dependent RNA Pol II phosphorylation via BRD4

Accession Numbers

GSE82243
GSE83228
GSE83230

Stratton et al., 2016, Cell Reports *16*, 1366–1378
August 2, 2016
http://dx.doi.org/10.1016/j.celrep.2016.06.074

OPEN ACCESS
CellPress

Cell Reports
Article

Signal-Dependent Recruitment of BRD4 to Cardiomyocyte Super-Enhancers Is Suppressed by a MicroRNA

Matthew S. Stratton,[1] Charles Y. Lin,[2] Priti Anand,[3] Philip D. Tatman,[1,4] Bradley S. Ferguson,[1] Sean T. Wickers,[1] Amrut V. Ambardekar,[1] Carmen C. Sucharov,[1] James E. Bradner,[5] Saptarsi M. Haldar,[3,6] and Timothy A. McKinsey[1,4,*]
[1]Division of Cardiology, Department of Medicine, University of Colorado Denver, Aurora, CO 80045, USA
[2]Department of Molecular and Human Genetics, Baylor College of Medicine, Houston, TX 77030, USA
[3]Gladstone Institute of Cardiovascular Disease, San Francisco, CA 94158, USA
[4]Medical Scientist Training Program, University of Colorado Denver, Aurora, CO 80045, USA
[5]Department of Medical Oncology, Dana-Farber Cancer Institute, Boston, MA 02215, USA
[6]Division of Cardiology, Department of Medicine and Cardiovascular Research Institute, UCSF School of Medicine, San Francisco, CA 94143, USA
*Correspondence: timothy.mckinsey@ucdenver.edu
http://dx.doi.org/10.1016/j.celrep.2016.06.074

SUMMARY

BRD4 governs pathological cardiac gene expression by binding acetylated chromatin, resulting in enhanced RNA polymerase II (Pol II) phosphorylation and transcription elongation. Here, we describe a signal-dependent mechanism for the regulation of BRD4 in cardiomyocytes. BRD4 expression is suppressed by microRNA-9 (miR-9), which targets the 3′ UTR of the *Brd4* transcript. In response to stress stimuli, miR-9 is downregulated, leading to derepression of BRD4 and enrichment of BRD4 at long-range super-enhancers (SEs) associated with pathological cardiac genes. A miR-9 mimic represses stimulus-dependent targeting of BRD4 to SEs and blunts Pol II phosphorylation at proximal transcription start sites, without affecting BRD4 binding to SEs that control constitutively expressed cardiac genes. These findings suggest that dynamic enrichment of BRD4 at SEs genome-wide serves a crucial role in the control of stress-induced cardiac gene expression and define a miR-dependent signaling mechanism for the regulation of chromatin state and Pol II phosphorylation.

INTRODUCTION

In response to diverse insults, the heart undergoes pathological remodeling, a process often characterized by cardiomyocyte hypertrophy, which contributes to contractile dysfunction and heart failure. Abnormalities in the control of gene expression are central to the pathogenesis of cardiac hypertrophy and heart failure (Kao et al., 2015; Lowes et al., 2002). A defined set of sequence-specific DNA-binding transcription factors (e.g., NFAT, GATA4, and MEF2) have been shown to be recruited to regulatory regions of the genome to trigger aberrant myocardial gene transcription by RNA polymerase II (Pol II) (Sano and Schneider, 2004; Sayed et al., 2013; van Berlo et al., 2013). Epigenetic events are also crucially involved in stress-dependent activation of pathological cardiac gene expression (Gillette and Hill, 2015; Mayer et al., 2015; Preissl et al., 2015; Renaud et al., 2015). For example, dynamic changes in N-ε-acetylation of lysine side chains on nucleosomal histone tails are observed during cardiac hypertrophy, and genetic and pharmacological manipulations of histone acetyltransferases and histone deacetylases have profound effects on pro-hypertrophic gene expression in cardiomyocytes (McKinsey, 2012; Xie and Hill, 2013).

Recently, a member of a family of epigenetic reader molecules called bromodomain and extraterminal (BET) acetyl-lysine binding proteins was shown to control pathological cardiac gene expression and cardiac hypertrophy (Haldar and McKinsey, 2014). JQ1, a first-in-class, potent, and specific inhibitor of BET bromodomains that functions by competitively displacing BET proteins from acetylated-histones (Filippakopoulos et al., 2010), was found to block agonist-dependent hypertrophy of cultured cardiomyocytes and also to inhibit pressure overload-mediated left ventricular (LV) hypertrophy in mice (Anand et al., 2013; Spiltoir et al., 2013). The anti-hypertrophic effect of JQ1 was recapitulated by genetic knockdown of a single BET family member, BRD4, implicating this reader protein as a nodal regulator of pathological gene expression in cardiomyocytes (Anand et al., 2013). BRD4 is thought to regulate cardiac gene expression through interactions with the positive transcription elongation factor b (P-TEFb) complex (Haldar and McKinsey, 2014). BRD4 associates with active, hyper-acetylated regions of regulatory chromatin via its acetyl-lysine recognition modules (bromodomains) and consequently activates Pol-II-dependent transcription through association with cyclin-dependent kinase 9 (CDK9), a key component of P-TEFb (Bisgrove et al., 2007; Jang et al., 2005; Yang et al., 2005). CDK9-mediated Pol II phosphorylation at transcription start sites (TSS) facilitates Pol II pause release and productive transcription elongation. In non-cardiac

cells, BRD4 has also been shown to disproportionately associate with a subset of cell state-specific enhancers called super-enhancers (SEs) (Brown et al., 2014; Chapuy et al., 2013; Di Micco et al., 2014; Lovén et al., 2013), which signal via long-range genomic interactions to regulate state-specific transcription programs from core promoters (Hnisz et al., 2013, 2015; Whyte et al., 2013).

The existence of BRD4-enriched SEs in cardiomyocytes has yet to be established. Furthermore, it is unclear whether BRD4 functions as a stress-responsive co-factor in the heart. Here, we define a microRNA (miR)-dependent signaling circuit in cardiomyocytes that controls dynamic recruitment of BRD4 to distinct genomic regulatory loci in response to pro-hypertrophic signals. In unstimulated cardiomyocytes, BRD4 protein abundance is restrained by miR-9. In response to stress stimuli, miR-9 expression is downregulated, allowing for selective targeting of BRD4 to cardiomyocyte SEs and promoters that regulate hypertrophic gene expression. Introduction of a miR-9 mimic into cardiomyocytes blunts signal-dependent recruitment of BRD4 to these *cis*-acting elements, leading to suppression of Pol II phosphorylation at associated TSSs and repression of downstream gene expression. In contrast, miR-9 does not alter BRD4 binding to SEs and promoters for constitutively expressed cardiac genes or genes that are downregulated in response to hypertrophic stimuli. These findings reveal an epigenetic signaling pathway that couples upstream cues to transcriptional outputs that drive pathological cardiac remodeling and heart failure pathogenesis.

RESULTS

miR-9 Targets BRD4 in Cardiomyocytes

We previously observed that increased BRD4 protein abundance during cardiac hypertrophy occurs without concomitant elevation of BRD4 mRNA (Anand et al., 2013; Spiltoir et al., 2013; Stratton and McKinsey, 2015), suggesting the possibility that cardiac BRD4 is post-transcriptionally controlled by a microRNA (miR). Indeed, in silico analysis of the *Brd4* mRNA 3′ UTR revealed four conserved binding sequences for six candidate miRs (miR-141, miR-200a, miR-124, miR-204, miR-211, and miR-9) (Figure 1A). We reasoned that a putative miR that targets BRD4 should be downregulated during hypertrophic stress (Figure 1B). As shown in Figure 1C, stimulation of neonatal rat ventricular myocytes (NRVMs) with the hypertrophic agonist phenylephrine (PE) failed to reduce expression of miR-141, miR-200a, miR-124, miR-204, or miR-211, arguing against roles for these miRs in the stress-coupled accumulation of BRD4 in the heart. In contrast, miR-9 was significantly downregulated in PE-treated cardiomyocytes in vitro (Figure 1C). Agonist-induced downregulation of miR-9 in cardiomyocytes was dependent on histone deacetylase (HDAC) catalytic activity (Figure 1D). miR-9 expression was also reduced in cultured cardiomyocytes stimulated with an independent hypertrophic agonist, prostaglandin F2α (PGF2α), and in vivo in rodent pressure overload models of left ventricular (LV) and right ventricular (RV) pathological cardiac hypertrophy (Figures 1E and 1F). In addition, mechanical unloading of failing human hearts with left ventricular assist devices (LVADs), which led to reversal of cardiac hypertrophy and improvement of systolic function in this patient cohort (Ambardekar et al., 2011), was associated with increased LV expression of miR-9, and this correlated with reduced levels of BRD4 protein in the myocardium (Figures 1G and 1H). The 7-mer-m8 target sequence for miR-9 in the *Brd4* 3′UTR is conserved in human, mouse, and rat (Figure 1I). Together, these data are consistent with the hypothesis that downregulation of miR-9 is a conserved mechanism for derepression of BRD4 in response to signals for pathological cardiac hypertrophy.

We next tested whether miR-9 could directly target BRD4. Transfection of miR-9 mimic into NRVMs led to a marked reduction of BRD4 protein abundance, which was comparable to the effect of directly targeting BRD4 transcripts with small interfering RNA (siRNA) (Figures 2A and S1A). Importantly, miR-9 mimic did not reduce expression of a closely related BET family member, BRD2, establishing the specificity of the observed decrease in BRD4 abundance. Conversely, blockade of endogenous miR-9 through transfection of a miR-9 inhibitor (anti-miR-9) into NRVMs increased endogenous BRD4 protein levels relative to control anti-miR, again without influencing BRD2 expression (Figure S1B). In addition, miR-9 mimic, but not control mimic, significantly reduced expression of a luciferase reporter harboring the 3′ UTR of rat *Brd4*, a silencing effect that was lost upon mutation of the conserved miR-9 target sequences in the 3′UTR (Figure 2B). Hence, miR-9 can directly suppress BRD4 protein abundance.

miR-9 and Small Molecule BET Bromodomain Inhibitor, JQ1, Target Overlapping Cardiac Gene Programs

Cardiomyocyte hypertrophy is blocked by the small molecule BET inhibitor, JQ1, or by genetic knockdown of BRD4 (Anand et al., 2013; Spiltoir et al., 2013). To address the hypothesis that JQ1 and miR-9 exert overlapping effects on cardiomyocyte gene expression via common targeting of BRD4, whole transcriptome analysis using RNA-seq was performed in NRVMs. NRVMs were transfected with miR-9 mimic or control mimic and were either left untreated or stimulated with PE for 48 hr (Figure 3A). Introduction of miR-9 mimic led to a significant reduction in NRVM hypertrophy (Figures 3B and 3C). Furthermore, the miR-9 mimic reversed many PE-mediated changes in gene expression, as illustrated by the heatmap (Figure 3D; Data S1). Comparison of changes in cardiomyocyte gene expression elicited by miR-9 mimic and JQ1 revealed significant overlap (Figure 3E). Functional pathway analysis demonstrated that a broad range of biological processes related to pathologic hypertrophy were similarly controlled by miR-9 and JQ1. Notably, the general patterns of reversing PE-induced growth and inflammation pathways, while rescuing expression of pathways associated with fatty acid oxidation metabolism, were observed (Data S2 and S3). As shown in Figure 3F, qPCR from independent samples confirmed that miR-9 mimic blunts expression of PE-inducible genes that are canonically associated with pathological cardiac hypertrophy (*Nppa*, *Nppb*, and *Xirp2*) and cardiac fibrosis (*Ctgf* and *TSC22D1*), consistent with observed effects of JQ1 (Anand et al., 2013; Spiltoir et al., 2013). PE-induced expression of these transcripts was also reduced in cardiomyocytes in which BRD4 expression was knocked down using short hairpin RNA (shRNA) (Figure S2).

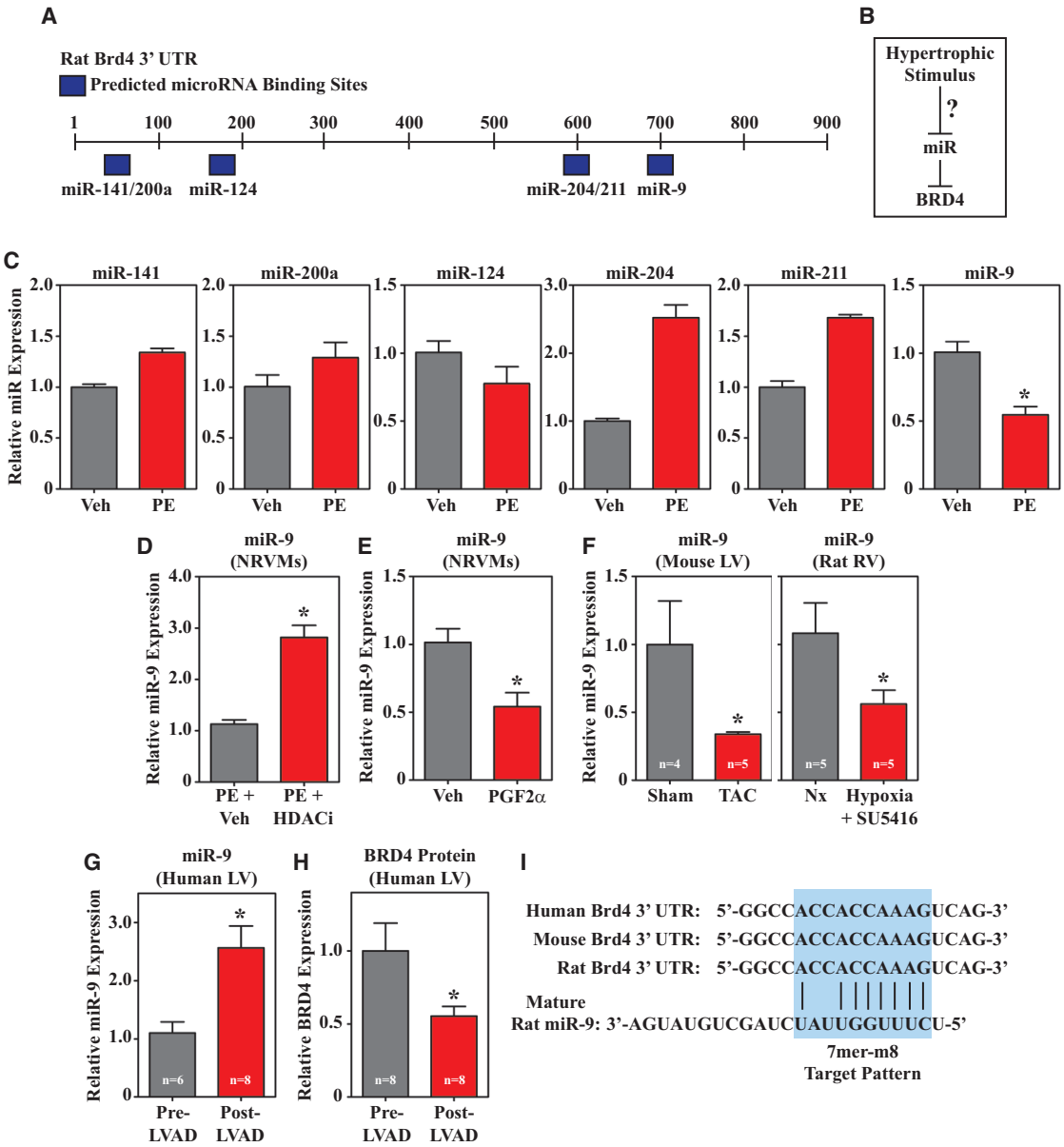

Figure 1. Cardiac miR-9 Expression Is Suppressed during Pathological Hypertrophy

(A) Schematic representation of the rat BRD4 3′UTR with predicted microRNA (miR) binding sites indicated.

(B) Hypothesis that signals for cardiac hypertrophy repress expression of a BRD4-targeting miR.

(C) Expression of putative BRD4 3′ UTR binding miRs in neonatal rat ventricular myocytes (NRVMs) treated with vehicle control (Veh) or the pro-hypertrophic agonist phenylephrine (PE; 10 μM) for 48 hr. Only miR-9 expression was significantly downregulated.

(D) Treatment with the histone deacetylase inhibitor (HDACi) AR-42 (500 nM) derepressed miR-9 expression in PE-treated NRVMs.

(E and F) miR-9 expression was also significantly downregulated in NRVMs treated with prostaglandin F2α (PGF2α; 10 μM) for 48 hr (E), in hypertrophic left ventricles (LV) of mice subjected to transverse aortic constriction (TAC), and in hypertrophic right ventricles (RV) of rats with pulmonary hypertension due to combined exposure to hypoxia and the VEGF receptor inhibitor SU5416 (F). *$p < 0.05$ versus vehicle or sham operated or normoxic (Nx) controls.

(G and H) Expression of miR-9 was significantly increased in human hearts upon mechanical unloading with a left ventricular assist device (LVAD) (G), which correlated with reduced BRD4 protein expression in the LV (H). *$p < 0.05$ versus Pre-LVAD.

(I) Conservation of the miR-9 binding site in human, mouse, and rat BRD4 3′UTR.

Together, these findings support the hypothesis that downregulation of miR-9 in response to a hypertrophic agonist allows for increased BRD4 activity, which subsequently promotes pathological cardiac gene expression.

Dynamic Recruitment of BRD4 to Cardiomyocyte Super-Enhancers Is Suppressed by miR-9

Although inhibition of BRD4 has defined a role for this protein as a positive regulator of cardiac hypertrophy, the extent to which

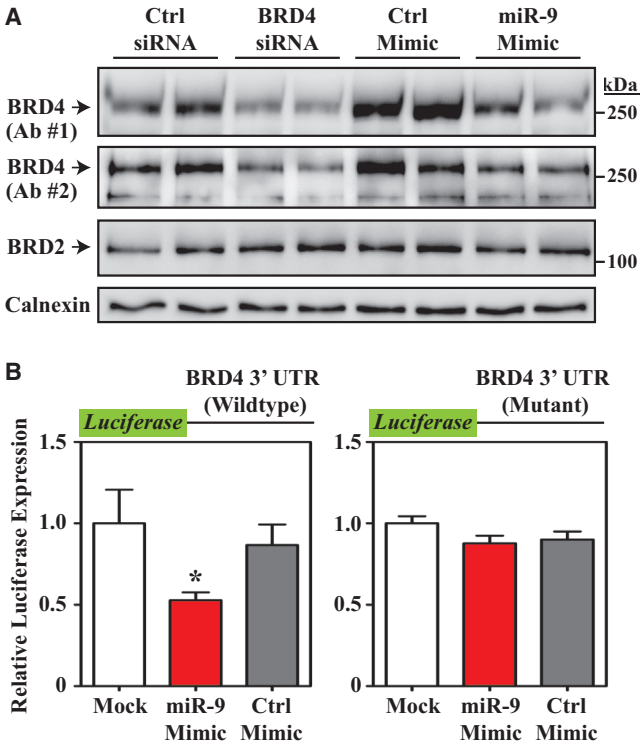

Figure 2. Cardiac BRD4 Expression Is Suppressed by miR-9

(A) NRVMs were transfected with the indicated siRNAs, microRNA mimics, microRNA inhibitors, or controls (Ctrl), and 48 hr post-transfection protein homogenates were analyzed by immunoblotting with the indicated antibodies; two independent anti-BRD4 antibodies were employed (Ab #1 and Ab #2), as described in the Experimental Procedures. The miR-9 mimic reduced expression of BRD4 as efficiently as a BRD4-targeting siRNA; calnexin served as a loading control.

(B) HEK293 cells were transfected with luciferase reporters fused to wild-type rat *Brd4* 3′ UTR or *Brd4* 3′UTR containing a point mutation at the miR-9 binding site. Cells were co-transfected with either miR-9 mimic or control, and luciferase activity was quantified 24 hr post-transfection. *$p < 0.05$ versus Ctrl mimic transfected cells.

See also Figure S1.

this chromatin reader is subject to signal-dependent control in cardiomyocytes is unclear. In particular, it is not known if genomic enrichment of cardiomyocyte BRD4 changes under hypertrophic stress, or whether it is affected by miR-9. To address these questions, we subjected NRVMs to whole-genome chromatin immunoprecipitation sequencing (ChIP-seq) to dynamically map gene regulatory elements bound by BRD4. NRVMs were transfected with miR-9 mimic or control mimic and were either left untreated or stimulated with PE for 48 hr. Chromatin immunoprecipitation (ChIP) was performed with a BRD4-specific antibody, and associated cardiomyocyte DNA was subject to deep sequencing (Figure 4A). Well-defined peaks of enhancer-associated BRD4 were mapped throughout the cardiomyocyte genome (Figure 4B). Aggregate analysis of the three treatment groups (unstimulated + control miR mimic, PE + control miR mimic and PE + miR-9 mimic) revealed prominent BRD4 binding to 3,771 gene enhancers, with enhancers defined as being at least 500 base pairs from the TSS of the associated gene.

To assess signal- and miR-9-dependent regulation of BRD4 genomic localization, subsequent analysis focused on SEs, which are long-range gene regulatory elements that have been defined in cancer and immune cells based on abundant BRD4 binding above a threshold level found at typical enhancers (TEs) (Brown et al., 2014; Chapuy et al., 2013; Lovén et al., 2013). Four hundred and fifty-nine BRD4-enriched SEs were detected in cardiomyocytes (Figure 4C). Cardiomyocyte SEs were ranked by change in BRD4 enrichment following PE treatment relative to unstimulated cells, and three general patterns of BRD4 dynamics were observed: (1) increased BRD4 binding with PE, (2) loss of BRD4 binding with PE, and (3) constitutive BRD4 binding that is unchanged by PE stimulation (Figure 4C). Using a 1.5-fold change threshold, BRD4 association was found to be increased at 65 SEs and reduced at 19 SEs in response to PE treatment (Figure 4D). miR-9 mimic blocked PE-mediated recruitment of BRD4 to SEs, while having no significant effect on agonist-dependent depletion of BRD4 from SEs or constitutive binding of BRD4 to basal SEs (Figures 4D and S3). BRD4 binding to SEs for the *Nppa*, *Nppb*, and *Ctgf* genes was dramatically enhanced by PE stimulation and blunted by miR-9 mimic, while high level constitutive binding of BRD4 to SEs for the *phospholamban* (*Pln*), and *myosin heavy chain* (*Myh*) *6/7* genes was unaffected by PE or miR-9 mimic (Figure 4E). These findings reveal the existence of dynamic BRD4-enriched SEs in cardiomyocytes and suggest that miR-9-regulated BRD4 protein is preferentially recruited to a subset of hyper-activated SEs in response to hypertrophic stimuli.

Bioinformatic analyses were performed to begin to address the mechanism by which hypertrophic agonists stimulate recruitment of BRD4 to distinct genomic loci in cardiomyocytes. Genome coordinates for the 65 SEs where BRD4 abundance was increased following PE treatment were enriched for AP-1 transcription factor family binding sites relative to randomly selected genomic sequences of similar length (Figure 5A). In contrast, there was no enrichment of AP-1 binding sites in SEs where BRD4 binding was reduced by PE treatment (not shown). To test the hypothesis that AP-1 transcription factors facilitate recruitment of BRD4 to SEs in response to hypertrophic agonists, we employed adenovirus encoding a mutant form of c-Fos that functions as a broad-spectrum dominant-negative inhibitor of the AP-1 family (dnAP-1) (Olive et al., 1997). SE1 and SE2 upstream of the *Ctgf* TSS (Figure 5B) were selected for anti-BRD4 ChIP-PCR analysis because they contain AP-1 binding sites and were bound by an increased amount of BRD4 upon PE treatment (Figure 4C). As shown in Figure 5C, BRD4 association with these SEs was significantly reduced in cardiomyocytes expressing dn-AP1 compared to control cells infected with adenovirus encoding β-galactosidase. Furthermore, diminished BRD4 targeting to SE1 and SE2 in dn-AP-1-expressing cardiomyocytes correlated with reduced expression of *Ctgf* mRNA, suggesting that AP-1-mediated recruitment of BRD4 to these sites is required for downstream target gene expression (Figure 5D).

miR-9 Blunts Stimulus-Dependent BRD4 Binding and Pol II Phosphorylation at Cardiac Gene Promoters

SEs are thought to signal to proximal promoters to stabilize BRD4-containing coactivator complexes near TSSs, thereby

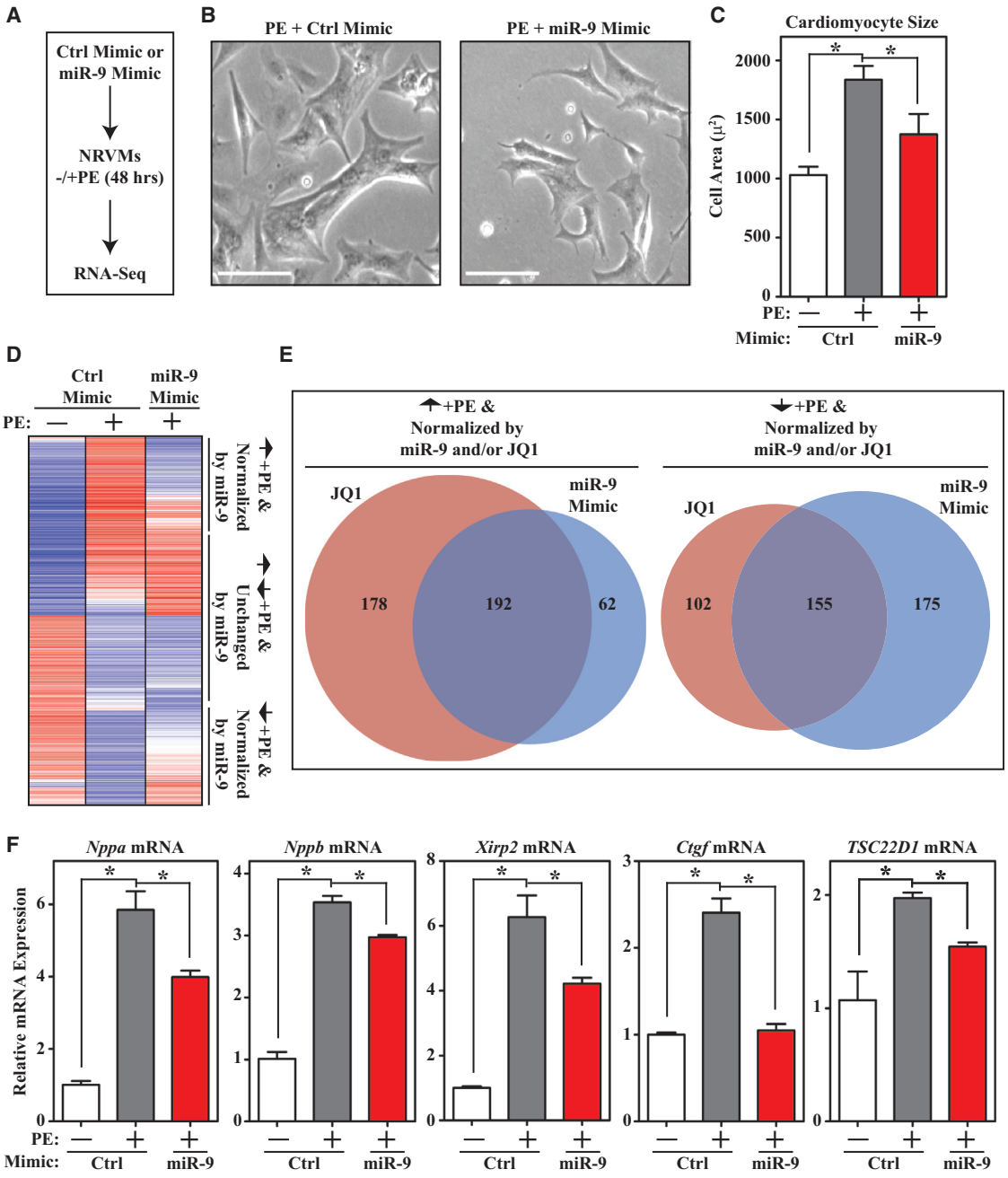

Figure 3. miR-9 and JQ1 Target Overlapping Gene Programs in Cardiomyocytes

(A) NRVMs were transfected with control mimic (Ctrl; 25 nM) or miR-9 mimic (25 nM), and 24 hr post-transfection cells were treated with vehicle (Veh) or phenylephrine (PE; 10 μM) for 48 hr. RNA was harvested for RNA-seq.

(B and C) NRVMs transfected with miR-9 mimic appeared smaller relative to controls (B), and quantitative assessment of cell size confirmed that miR-9 mimic significantly blunted PE-induced hypertrophy (C) (n = 24 per group; *p < 0.05 versus Ctrl). Scale bar, 100 μm.

(D) Heatmap summary of NRVM gene expression in the indicated treatment groups. Gene expression patterns were categorized based on responses to PE and miR-9 mimic.

(E) miR-9 mimic-dependent gene expression changes were compared to changes seen with BET protein inhibition using JQ1. The Venn Diagrams indicate significant alterations in gene expression mediated by miR-9 mimic and JQ1 treatment, with both treatments blunting induction of gene expression by PE, and rescuing expression of genes that are suppressed by PE.

(F) qPCR confirmed that miR-9 mimic inhibits PE-induced expression of prototypical pathological cardiac genes (n = 3 per treatment group; *p < 0.05).

See also Figure S2 and Data S1, S2, and S3.

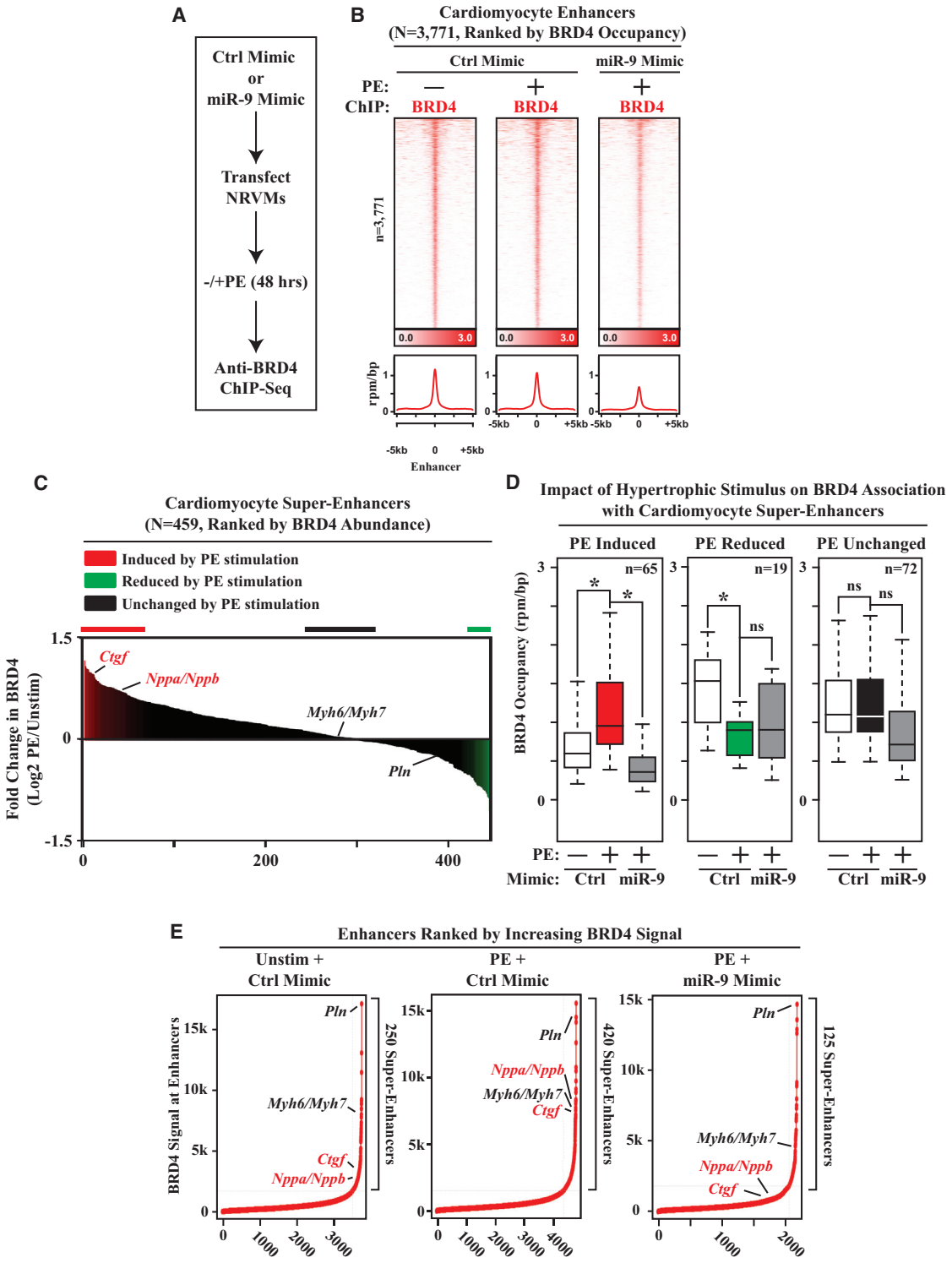

Figure 4. Signal-Dependent Recruitment of BRD4 to Cardiomyocyte Gene Super-Enhancers Is Blunted by miR-9

(A) NRVMs were transfected with control mimic (Ctrl; 25 nM) or miR-9 mimic (25 nM), and 24 hr post-transfection cells were treated with vehicle (Veh) or phenylephrine (PE; 10 μM) for 48 hr. Hi-seq DNA sequencing was conducted on NRVM chromatin immunoprecipited with a BRD4-specific antibody.

(B) A total of 3,771 BRD4-enriched cardiomyocyte enhancers were identified, as defined by a distance of >500 bp from proximal promoters and are graphed in heatmap format by treatment group. Each row shows ±5 kb centered on the BRD4 peak, with rows ordered by max BRD4 signal in each region. miR-9 mimic reduced the summed absolute BRD4 signal (rpm/bp) at enhancers, as shown below the heatmap.

(legend continued on next page)

A

PE Induced Super-Enhancers	
Motif Name	*P*-Value
Jun-AP1 (bZIP)	1.00E-07
Jun-CRE (bZIP)	1.00E-07
CArG (MADS)	1.00E-07
Fosl2 (bZIP)	1.00E-06
BATF (bZIP)	1.00E-04
Mef2c (MADS)	1.00E-04
Fra1 (bZIP)	1.00E-04
Mef2a (MADS)	1.00E-04
TEAD2 (TEA)	1.00E-03
Atf2 (bZIP)	1.00E-03
AP-1 (bZIP)	1.00E-03
Atf7 (bZIP)	1.00E-03
Atf3 (bZIP)	1.00E-03
JunD (bZIP)	1.00E-02

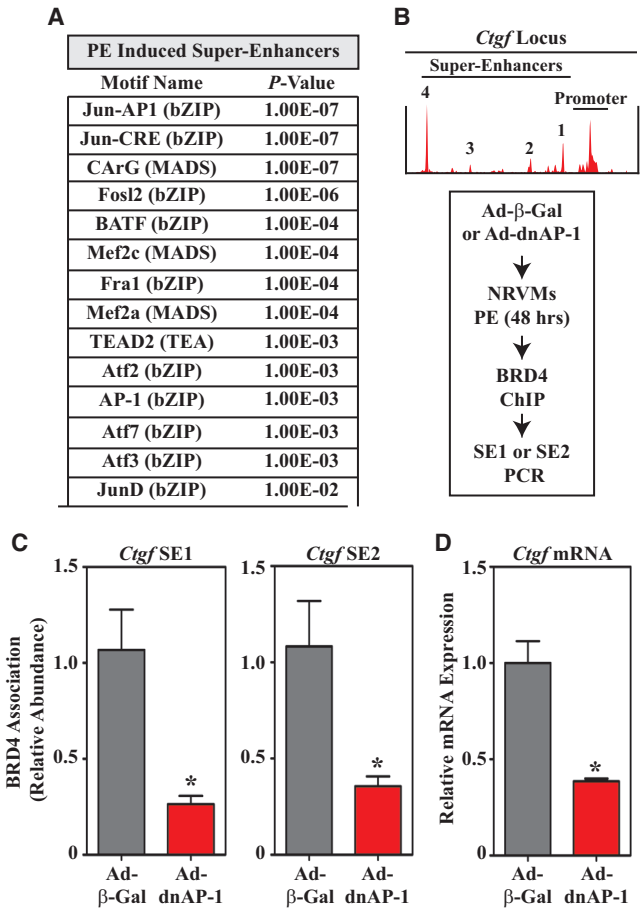

Figure 5. AP-1 Function Is Required for Stimulus-Coupled Recruitment of BRD4 to *Ctgf* SEs

(A) Analysis of PE-inducible, BRD4-enriched SE sequences revealed enrichment of the indicated, predicted transcription factor binding sites. Binding sites for members of the AP-1 transcription factor family were over-represented.

(B) To test the hypothesis that AP-1 facilitates recruitment of BRD4 to SEs for pro-hypertrophic genes, NRVMs were infected with adenoviruses encoding dominant-negative AP-1 (Ad-dnAP-1) or β-galactosidase control (Ad-β-Gal). After 48 hr of PE treatment, sheared chromatin was subjected to anti-BRD4 ChIP, followed by PCR to quantify the presence of SE1 and SE2 of the *Ctgf* locus, as indicated.

(C and D) Expression of dnAP-1 significantly reduced the abundance of BRD4 at these SEs (C), which correlated with suppression of *Ctgf* mRNA expression (D). *$p < 0.05$ versus Ad-β-Gal.

facilitating p-TEFb-mediated Pol II phosphorylation and transcription elongation (Arner et al., 2015; Brown et al., 2014; Pnueli et al., 2015). ChIP-seq data were further analyzed to assess whether PE and/or miR-9 alter BRD4 binding to cardiomyocyte gene promoters. To define promoters, ChIP-seq was performed with a total Pol II-specific antibody. Upon overlay of the BRD4 ChIP-seq data, 422 cardiomyocyte promoters were found to be co-occupied by Pol II and BRD4. Similar to SE analysis, three general patterns of BRD4 dynamics were observed at gene promoters: (1) increased BRD4 binding with PE, (2) loss of BRD4 binding with PE, and (3) constitutive BRD4 binding that is unchanged by PE stimulation (Figure 6A). BRD4 binding to cardiomyocyte promoters was significantly altered by miR-9 mimic (Figure 6B). Indeed, ChIP-seq gene tracks illustrate PE-inducible BRD4 binding to the promoters for the *Nppa*, *Nppb*, and *Ctgf* genes, and reduction of BRD4 binding to these sites in cells transfected with miR-9 mimic (Figure 6C). Consistent with the SE analysis, BRD4 binding to the promoter of constitutively expressed *Pln* was unaffected by either PE or miR-9 (Figure 6D).

ChIP-PCR studies were next performed to test the hypothesis that the miR-9-mediated reduction of BRD4 enrichment leads to suppression of Pol II phosphorylation at corresponding TSSs. NRVMs were transfected with miR-9 mimic or control mimic and were either left unstimulated or stimulated with PE. After 48 hr of stimulation, ChIP was performed with an antibody specific for phospho-Ser-2 of the C-terminal domain of Pol II, which reflects locus-specific enrichment for this elongating phosphoform. DNA was analyzed by qPCR with primers flanking the TSSs at the *Nppa*, *Nppb*, and *Ctgf* loci (Figure 7A). PE-mediated Ser 2P-Pol II enrichment at these sites was significantly reduced by miR-9 mimic (Figure 7B), consistent with the ability of miR-9 to suppress agonist-mediated gene induction (see Figure 3F) and BRD4 enrichment at associated SEs (Data S4). Together, these findings suggest that miR-9 blunts signal-dependent pathological cardiac gene induction by repressing BRD4-dependent Pol II phosphorylation and transcription elongation.

DISCUSSION

The mechanisms by which stress stimuli are coupled to epigenetic events that drive heart failure pathogenesis remain poorly defined. Here, we describe a pathway for the inducible formation of BRD4-enriched cardiomyocyte SEs, which function as signal-integrating platforms to trigger pathological gene expression via induction of Pol II phosphorylation. Signal-dependent targeting of BRD4 to distinct genomic loci in cardiac muscle requires HDAC-mediated downregulation of miR-9, establishing a role for a microRNA in the genesis of SEs and in RNA Pol II activation in the heart.

Our data suggest the presence of at least three pools of BRD4, only one of which is significantly influenced by miR-9. Newly accumulated, miR-9-regulatable BRD4 appears to be the

(C) A total of 459 SEs, defined by BRD4 signal breadth and intensity, are plotted on the x axis and ranked by log2 fold change upon PE treatment.

(D) Box plots of BRD4 binding to SEs, categorized as PE-induced, PE-reduced, or PE-unchanged based on 1.5-fold change (induced, reduced) or <0.05-fold change (unchanged). miR-9 mimic blunted BRD4 recruitment to PE-induced SEs without significantly altering binding to constitutive (unchanged) SEs. miR-9 also failed to significantly attenuate PE-mediated release of BRD4 binding from certain SEs. *$p < 0.05$.

(E) Enhancers and SEs were ranked by BRD4 signal intensity. PE treatment dramatically enhanced BRD4 binding to SEs associated with the *Nppa*/*Nppb* and *Ctgf* genes, and miR-9 mimic blocked BRD4 recruitment to these SEs. BRD4 binding to SEs for the *phospholamban* (*PLN*), and *Myh6*/*Myh7* genes were not significantly altered by PE or miR-9 mimic.

See also Figure S4 and Data S4.

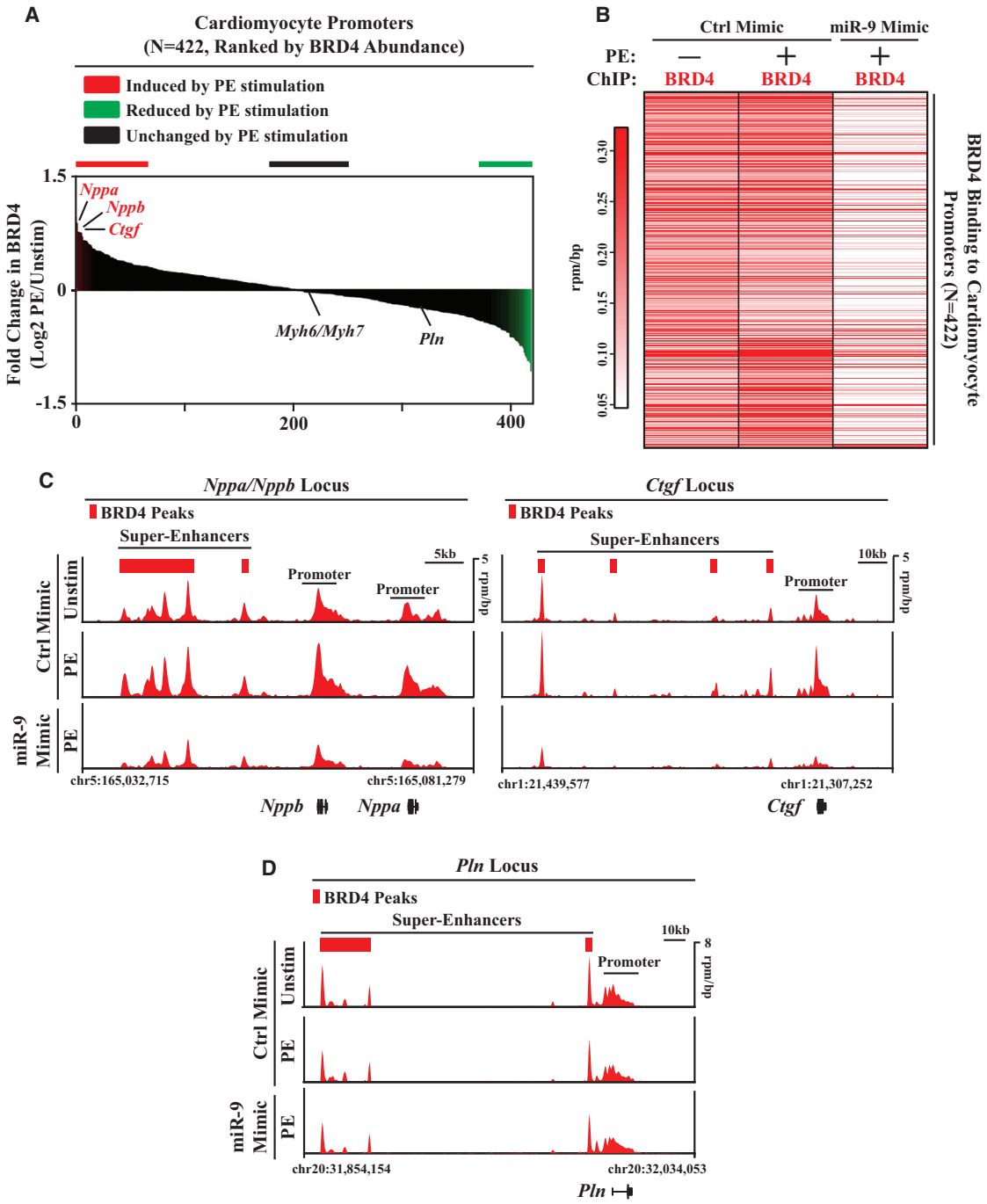

Figure 6. miR-9 Mimic Blunts Stimulus-Coupled Recruitment of BRD4 to Active Cardiomyocyte Promoters

(A) Promoters were defined in NRVMs based on Pol II and BRD4 co-occupancy. 420 BRD4-bound promoters are plotted on the x axis and ranked by log2-fold change in BRD4 enrichment upon PE treatment (relative to control mimic + vehicle treatment). PE treatment led to BRD4 recruitment to *Nppa*, *Nppb*, and *Ctgf* promoters without affecting BRD4 recruitment to *Myh6*/*Myh7* or *Pln* promoters.

(B) BRD4-enriched active cardiomyocyte promoters are depicted in heatmap format. Red intensity indicates increased BRD4 signal relative to median intensity.

(C and D) Stimulus-coupled recruitment of BRD4 to SEs and promoters is illustrated by the BRD4 ChIP-seq tracks at the *Nppb*, *Nppa*, and *Ctgf* (C) gene loci. miR-9 mimic diminished BRD4 binding to regulatory regions for each of these genes. BRD4 binding to the SE and promoter of the constitutively expressed *Pln* gene (D) was unaffected by either PE or miR-9.

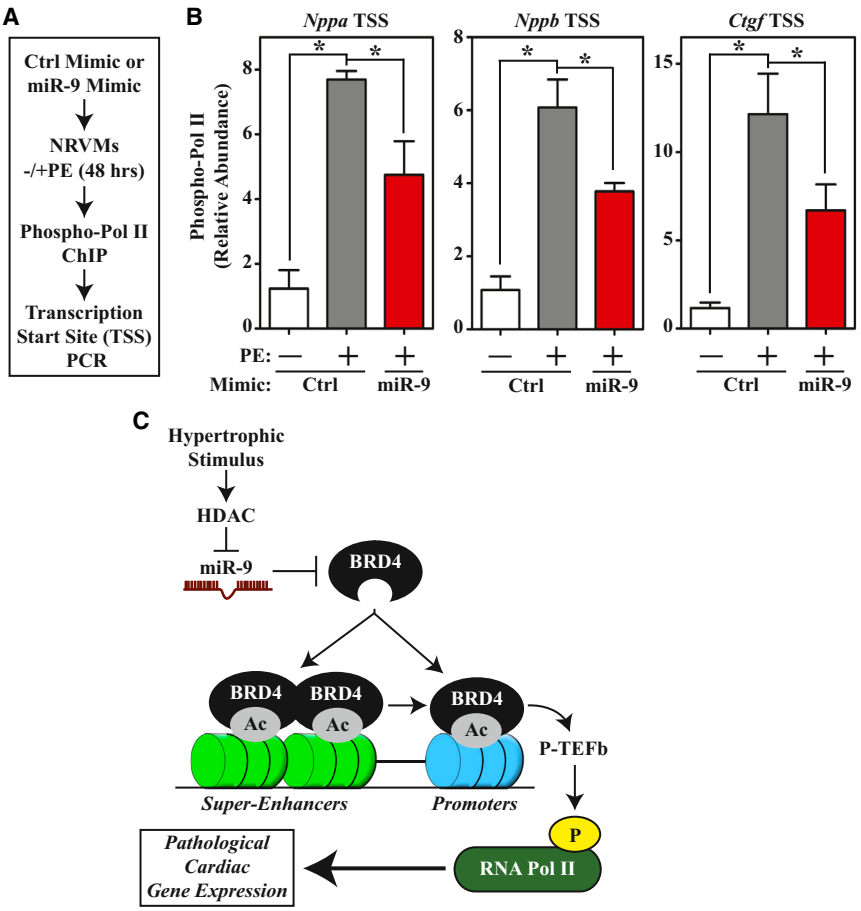

Figure 7. miR9 Suppresses Signal-Dependent Pol II Phosphorylation at Transcription Start Sites of Genes Associated with Pathologic Hypertrophy

(A) Experimental design for ChIP-PCR studies of Pol II phosphorylation at the transcription start sites (TSSs) for the *Nppa*, *Nppb*, and *Ctgf* genes.

(B) PE-mediated Pol II phosphorylation at each of these sites was significantly inhibited by miR-9. *$p < 0.05$. Note the correlation between changes in Pol II phosphorylation and expression of these genes (Figure 3F).

(C) A model for stimulus-dependent regulation of pathological cardiac gene expression by miR-9 and BRD4.

predominant form that is dynamically recruited to activated SEs in response to a hypertrophic stimulus. In contrast, large peaks of BRD4 on SEs associated with constitutively expressed genes (e.g., *Pln*) are unaffected by miR-9, and signal-dependent release of BRD4 from existing basal SEs is not blocked by miR-9. Thus, miR-9 selectively blunts the augmented, signal-induced pool of BRD4 that is targeted to SEs and promoters of genes that are activated during pathological hypertrophy, rather than functioning as a global suppressor of BRD4 function.

Signal-dependent formation of BRD4-enriched SEs in cardiomyocytes is distinct from SE remodeling in endothelial cells (Brown et al., 2014). In cardiomyocytes, increased abundance of BRD4 in response to a hypertrophic agonist facilitates excess loading of BRD4 onto SEs, whereas TNFα treatment of endothelial cells leads to nuclear factor κB (NF-κB)-dependent redistribution of BRD4 from basal SEs to de novo, stress-activated SEs. Furthermore, endothelial cell activation results in a reduction in the overall number of SEs, while hypertrophic stimulation of cardiomyocytes leads to a significant increase of BRD4-bound SEs. Recruitment of BRD4 to discrete genomic loci in cardiomyocytes likely involves associations with DNA binding transcription factors and/or formation of an underlying histone code that is preferentially bound by BRD4 (Brown et al., 2014; Dey et al., 2003; Filippakopoulos et al., 2012; Hnisz et al., 2015; Shi et al., 2014; Wu et al., 2013). With regard to the former mechanism, we have found that recruitment of BRD4 to SEs that lie upstream of the *Ctgf* TSS is mediated, at least in part, by members of the AP-1 family of transcription factors (Figure 5). Further granularity on the molecular underpinnings of dynamic SE formation in the heart will accompany delineation of additional components of BRD4-enriched genomic complexes in cardiomyocytes.

It is possible that BRD4 is controlled by small RNA molecules other than miR-9. For example, the abundance of an ~150 kDa form of BRD4 was recently shown to be influenced by miR-204 in lung vascular smooth muscle cells (Meloche et al., 2015). However, hypertrophic stimulation of cardiomyocytes does not reduce miR-204 expression (Figure 1C), arguing against a role for this non-coding RNA in the control of BRD4 in the heart. It is intriguing to speculate that miR-9 targeting of BRD4 provides a generalizable mechanism for the regulation of chromatin signaling that extends beyond heart muscle to tissues such as brain, where both miR-9 and BRD4 serve crucial roles in the control of neural gene expression (Korb et al., 2015; Yuva-Aydemir et al., 2011).

The capacity of miRs to modulate complex pathophysiological processes, including heart failure, is attributed to their ability to target broad collections of mRNAs (Olson, 2014; van Rooij and Olson, 2012). As such, changes in cardiac gene expression elicited by miR-9 are likely due to both BRD4-dependent and BRD4-independent effects. In this regard, a miR-9 mimic was shown to exhibit a high degree of efficacy and tolerability in a mouse model of β-adrenergic receptor-mediated cardiac remodeling (Wang et al., 2010). Anti-hypertrophic activity of miR-9 in this model was linked to reduced expression of myocardin, a transcriptional co-activator that promotes hypertrophy through association with serum response factor (SRF) (Xing et al., 2006). Although determination of the relative contribution of SRF versus BRD4 downregulation to overall changes in cardiac gene expression imparted by miR-9 awaits future study, it

is likely that BRD4 targeting by miR-9 influences a more wide-ranging constellation of genes via effects on chromatin signaling and Pol II dynamics. This notion is supported by the similarity in transcriptome-wide gene expression changes in cardiomyocytes treated with miR-9 mimic or the small molecule BET inhibitor, JQ1 (Figure 3E).

Fibrosis is another key component of heart failure, and it should be noted that many of the BRD4-enriched SEs we identified in cardiomyocytes are associated with pro-fibrotic genes, including those encoding the secreted factors CTGF, plasminogen activator inhibitor-1 (PAI-1/Serpine1) and transforming growth factor beta-2 (TGF-β2) (Data S4). These findings suggest the possibility that miR-9/BRD4 signaling in cardiomyocytes regulates expression of paracrine factors that crosstalk with fibroblasts in the heart to elicit fibrotic remodeling. Furthermore, the prospect of miR-9/BRD4 directly regulating pro-fibrotic gene expression in cardiac fibroblasts warrants future consideration, especially in light of the recent discovery that miR-9 exhibits anti-fibrotic effects in the lung (Fierro-Fernández et al., 2015).

Our prior studies demonstrated that general BET inhibition with JQ1 blocks Pol II phosphorylation and transcriptional pause release of Pol II in response to pathological stress in the heart (Anand et al., 2013; Spiltoir et al., 2013). Here, we provide evidence of a molecular circuit for stress-dependent control of Pol II dynamics at TSSs of genes that promote adverse cardiac remodeling. The circuit is activated upon signal- and HDAC-dependent repression of miR-9, which enables BRD4 enrichment at SEs and promoters of pro-hypertrophic genes and leads to subsequent Pol II phosphorylation and transcription elongation (schematized in Figure 7C). Manipulation of this chromatin signaling axis may provide an innovative avenue for the treatment of cardiovascular disease.

EXPERIMENTAL PROCEDURES

RNA-Seq and ChIP-Seq

RNA was isolated from NRVMs using the High Pure RNA Isolation Kit (Roche). RNA was submitted to the WITG for library preparation (TruSeq Stranded mRNA Library Prep Kit, Illumina) and sequencing (HighSeq 2500). All RNA sample had 260/280 ratios above 2.1 and Rin scores above 8. ChIP was conducted with cultured NRVMs as previously reported (Anand et al., 2013). Detailed descriptions of the methods employed for ChIP and for analysis of RNA-seq and ChIP-seq data are described below.

ChIP and ChIP-Seq

Chromatin was crosslinked in 1% PFA for 10 min and unreacted PFA was neutralized with glycine for 5 min, washed with ice cold PBS, and harvested in PBS with protease and phosphatase inhibitors (Halt). NRVM pellets were snap frozen and stored at −80°C until processed. Pellets were re-suspended in lysis buffer 1 (50 mM HEPES, 140 mM NaCl, 1 mM EDTA, 10% glycerol, 0.5% NP40, 0.25% Triton X-100) and rotated for 15 min at 4°C. After centrifugation, pellets were then re-suspended in lysis buffer 2 (10 mM Tris HCl, 200 mM NaCl, 1 mM EDTA, 0.5 mM EGTA) and rotated for 5 min at 4°C. After centrifugation, pellets were re-suspended in shearing buffer (50 mM HEPES, 140 mM NaCl, 1 mM EDTA, 1 mM EGTA, 1% TX100, 0.1% sodium deoxycholate, 1% SDS) and sheared using a Diagenode Bioruptor (15 min, 30 s on/30 s off, setting high). Cleared chromatin was then immunoprecipitated with 5 μg of antibody attached to protein G Dynabeads (Invitrogen). Thirty million cells were used per ChIP for BRD4 (Bethyl, A301-985A) ChIP-seq and 15,000,000 cells were used per ChIP for RNA Pol II (Santa Cruz N-20, sc-899) ChIP-seq. Following overnight immunoprecipitation (IP), beads were washed five times and DNA was eluted in 50 mM Tris HCl, 10 mM EDTA, and 1% SDS solution at 65°C for 15 min. Following reversal of crosslinks, RNase, and proteinase treatment, DNA was purified using the MinElute PCR Purification kit (QIAGEN). Minor modifications were made to the above protocol for ChIP qPCR investigation of RNA Pol II phosphorylation on serine 2 (Abcam, ab24758). ChIP-seq DNA was submitted to WITGC for library preparation (TruSeq ChIP Sample Prep Kit for ChIP-Seq, Illumina) and sequencing (HighSeq 2500).

Sequencing Data Analysis

All analysis was performed using Rat RN4 genome and RN4 RefSeq gene annotations. Raw and processed ChIP-seq and RNA-seq data were deposited to the GEO online database (http://www.ncbi.nlm.nih.gov/geo/) under accession numbers GEO: GSE82243 and GSE83228.

RNA-Seq Processing

All RNA-seq datasets were aligned to the transcriptome using Tophat2 (version 2.0.11) (http://www.genomebiology.com/2013/14/4/R36/abstract). Gene expression values were quantified using Cufflinks and Cuffnorm (version 2.2.0) (Trapnell et al., 2010).

ChIP-Seq Processing

All ChIP-seq datasets were aligned using Bowtie2 (version 2.2.1) to build version RN4 of the rat genome (Langmead and Salzberg, 2012). Alignments were performed using the following criteria: -k 1. These criteria preserved only reads that mapped uniquely to the genome. ChIP-seq read densities were calculated the normalized using Bamliquidator (https://github.com/BradnerLab/pipeline/wiki/Bamliquidator). Briefly, ChIP-seq reads aligning to the region were extended by 200 base pairs (bp) and the density of reads per bp was calculated. The density of reads in each region was normalized to the total number of million mapped reads producing read density in units of reads per million mapped reads per bp (rpm/bp). MACS version 1.4.2 (model-based analysis of ChIP-seq) peak finding algorithm was used to identify regions of ChIP-seq enrichment over background (Zhang et al., 2008). A p value threshold of enrichment of 1e-9 was used for all datasets. A gene was defined as actively transcribed if enriched regions for RNA polymerase II (RNA Pol II) were located within ±1 kb of the TSS.

Mapping and Comparing Enhancers and Super-Enhancers

BRD4 ChIP-seq data were used to identify active *cis*-regulatory elements in the genome. ROSE2 (https://github.com/bradnerlab/pipeline/) was used to identify BRD4 enhancers and super-enhancers as in Brown et al. (2014). Briefly, proximal regions of BRD4 enrichment were stitched together if within 2 kb of one another. This 2 kb stitching parameter was determined by ROSE2 as the distance that optimally consolidated the number of discreet enriched regions in the genome while maintaining the largest fraction of enriched bases per region. Comparison of BRD4 changes at enhancers, super-enhancers, and promoter regions was performed as previously described (Brown et al., 2014). Active genes within 50 kb of enhancer regions were assigned as target genes, as described previously (Brown et al., 2014).

Transcription Factor Binding Site Analysis

Genomic DNA sequences of BRD4 SEs from the RN4 reference genome were searched for TF binding sites using LASAGNA 2.0. Reference TF binding sites were taken from the Citrome server, Encode, and the Transfac database.

qPCR

For assessment of miR expression, cDNA was prepared using miScript II RT kit (Hi Flex buffer option, QIAGEN) from Trizol-isolated RNA. qPCR was accomplished with miScript SYBR Green PCR kit (QIAGEN) using a StepOnePlus Real-Time PCR System (Life Technologies). For assessment of pathological hypertrophy markers, cDNA was prepared using Verso cDNA Synthesis Kit (Life Technologies) from Trizol-isolated RNA. qPCR was accomplished with DyNAmo Flas SYBR Green qPCR kit (Life Technologies) using a StepOnePlus Real-Time PCR System (Life Technologies). Primer sequences are shown in Table S1. Sham and TAC LVs, Nx, and Hypoxia + SU5416 RVs, and human pre- and post-LVAD samples have been previously described (Ambardekar

et al., 2011; Cavasin et al., 2014; Spiltoir et al., 2013; Stratton and McKinsey, 2015; Weitzel et al., 2013). Relative gene expression was calculated using the –ΔΔCt method with normalization to 18S.

Protein Analysis

Protein lysates were prepared in RIPA buffer containing Halt Protease Phosphatase Inhibitor cocktail (ThermoScientific; 1861280). Cells were sonicated prior to clarification by centrifugation. Protein concentrations were determined using a BCA Protein Assay Kit (Thermo Scientific). Proteins were resolved by SDS-PAGE, transferred to nitrocellulose membranes (Life Science Products) and probed with primary antibodies specific for calnexin (Santa Cruz Biotechnology, sc-11397), BRD2 (Cell Signaling Technology; #5848), BRD4 (Bethyl Laboratories, A301-985A; Ab #1), or BRD4 (Abcam, ab128874; Ab #2). Proteins were detected using SuperSignal West Pico Chemiluminescent Substrate (ThermoScientific; 34080) and a FluorChem HD2 Imager (Alpha Innotech). The Colorado Multicenter Institutional Review Board approved the protocol for the collection, storage, and analysis of human tissue.

Luciferase Assays

The 3′UTR of rat BRD4 was PCR-amplified from NRVM cDNA and cloned into the pmirGLO Dual-Luciferase miRNA Target Expression Vector (Promega). Mutant BRD4 3′ UTR was generated by site-directed mutagenesis PCR. One microgram of reporter construct and miR mimic (25 nM final concentration) was transfected into HEK293 cells using LIPO3000 transfection reagent. After 24 hr, cells were harvested and assayed using the Dual-Luciferase Reporter Assay System (Promega). Luciferase/Renilla activity was measured on a Glomax 20/20 Luminometer.

NRVM Isolation, Culture, and Adenovirus Infection

Neonatal rat ventricular myocytes (NRVMs) were isolated from the hearts of 1- to 3-day-old Sprague-Dawley rats (Charles River), as previously described (Simpson et al., 1989). Cell counting and viability was assayed using a Vi-Cell Cell Viability Analyzer (Beckman Coulter). Cells were incubated overnight on 10-cm plates coated with 0.2% gelatin (Sigma-Aldrich; G9391) in DMEM with 5% calf serum, 2 mM L-glutamine, and penicillin-streptomycin. The following morning, cells were washed with serum-free medium and maintained in DMEM supplemented with L-glutamine, penicillin-streptomycin, and Neutridoma-SP (0.1%; Roche Applied Science), which contains albumin, insulin, transferrin, and other defined organic and inorganic compounds. For all studies, cells were treated in maintenance media for 48 hr in the absence or presence of agonists. PE, PGF2α, and AR-42 were obtained from Sigma, Enzo Life Sciences, and Selleckchem, respectively.

NRVMs were treated with the following miR mimics, miR inhibitors, and siRNAs: miRIDIAN microRNA Rat rno-miR-9a-5p Mimic (Dharmacon), miRIDIAN microRNA Rat rno-miR-9a-5p–Hairpin Inhibitor (Dharmacon), miRIDIAN microRNA Hairpin Inhibitor Negative Control #2 (Dharmacon) mission siRNA for BRD4 SASI_RN02_00315747 (Sigma Aldrich), and mission siRNA Universal Negative Control #1 (Sigma-Aldrich).

Adenoviruses encoding dnAP-1, shBRD4, and shControl were previously described (Anand et al., 2013; Olive et al., 1997). NRVMs were infected at the time of plating with a multiplicity-of-infection of 50, and washed after overnight incubation.

Quantification of NRVM Cell Size

NRVM images were captured on the EVOS FL Cell Imaging System (Thermo Fisher Scientific). Cell size was quantified in Image J by a researcher blinded to treatment group. Each treatment group contained three independent plates of NRVMs. Two fields of view per plate were selected at random and four cells per field were measured after size calibration.

Statistical Analysis

All data (except RNA-seq and ChIP-seq) were analyzed with GraphPad Prism using either t tests (unpaired, two-tailed) when two variables were present, or ANOVA (one-way with posthoc) when three variables were present. Error bars represent ± SEM.

ACCESSION NUMBERS

The accession number for the ChIP-seq data reported in this paper is GEO: GSE82243. The accession numbers for the RNA-seq data and publication series reported in this paper are GEO: GSE83228 and GSE83230, respectively.

SUPPLEMENTAL INFORMATION

Supplemental Information includes Supplemental Experimental Procedures, three figures, one table, and four data files and can be found with this article online at http://dx.doi.org/10.1016/j.celrep.2016.06.074.

AUTHOR CONTRIBUTIONS

Conceptualization, M.S.S., T.A.M., and S.M.H.; Methodology, C.C.S.; Software, C.Y.L.; Formal Analysis, C.Y.L. and P.D.T.; Investigation, M.S.S., C.Y.L., P.A., B.S.F., P.D.T., and S.T.W.; Resources, A.V.A.; Data Curation, C.Y.L. and P.D.T.; Writing – Original Draft, M.S.S. and T.A.M.; Writing – Reviewing and Editing, M.S.S., T.A.M., C.Y.L., S.M.H., J.E.B., A.V.A., and C.C.S.; Funding Acquisition, M.S.S., T.A.M., J.E.B., and S.M.H.

ACKNOWLEDGMENTS

We thank miRagen Therapeutics for the control mimic, members of the K. Song lab for assistance with microscopy, and C. Vinson (NCI) for Ad-dnAP-1/AFos. This work was supported by NIH R01HL127240 (to J.E.B., S.M.H., and T.A.M.). T.A.M. was also supported by the NIH (R01HL116848 and R21AG043822) and the American Heart Association (Grant-in-Aid 14510001). S.M.H. was also supported by NIH DK093821. M.S.S. was funded by a T32 training grant and an F32 fellowship from the NIH (5T32HL007822 and F32HL126354). C.Y.L. is supported by a US Department of Defense CDMRP CA120184 postdoctoral fellowship. A.V.A. is supported by a Scientist Development Grant (from the American Heart Association) and the Boettcher Foundation's Webb-Waring Biomedical Research Program. The REDCap database used in the maintenance of the human cardiac tissue bank was supported by NIH/NCATS Colorado CTSA grant UL1 TR001082.

Received: November 16, 2015
Revised: May 4, 2016
Accepted: June 16, 2016
Published: July 14, 2016

REFERENCES

Ambardekar, A.V., Walker, J.S., Walker, L.A., Cleveland, J.C., Jr., Lowes, B.D., and Buttrick, P.M. (2011). Incomplete recovery of myocyte contractile function despite improvement of myocardial architecture with left ventricular assist device support. Circ Heart Fail *4*, 425–432.

Anand, P., Brown, J.D., Lin, C.Y., Qi, J., Zhang, R., Artero, P.C., Alaiti, M.A., Bullard, J., Alazem, K., Margulies, K.B., et al. (2013). BET bromodomains mediate transcriptional pause release in heart failure. Cell *154*, 569–582.

Arner, E., Daub, C.O., Vitting-Seerup, K., Andersson, R., Lilje, B., Drabløs, F., Lennartsson, A., Rönnerblad, M., Hrydziuszko, O., Vitezic, M., et al.; FANTOM Consortium (2015). Transcribed enhancers lead waves of coordinated transcription in transitioning mammalian cells. Science *347*, 1010–1014.

Bisgrove, D.A., Mahmoudi, T., Henklein, P., and Verdin, E. (2007). Conserved P-TEFb-interacting domain of BRD4 inhibits HIV transcription. Proc. Natl. Acad. Sci. USA *104*, 13690–13695.

Brown, J.D., Lin, C.Y., Duan, Q., Griffin, G., Federation, A.J., Paranal, R.M., Bair, S., Newton, G., Lichtman, A.H., Kung, A.L., et al. (2014). NF-κB directs dynamic super enhancer formation in inflammation and atherogenesis. Mol. Cell *56*, 219–231.

Cavasin, M.A., Demos-Davies, K.M., Schuetze, K.B., Blakeslee, W.W., Stratton, M.S., Tuder, R.M., and McKinsey, T.A. (2014). Reversal of severe angioproliferative pulmonary arterial hypertension and right ventricular hypertrophy

by combined phosphodiesterase-5 and endothelin receptor inhibition. J. Transl. Med. *12*, 314.

Chapuy, B., McKeown, M.R., Lin, C.Y., Monti, S., Roemer, M.G., Qi, J., Rahl, P.B., Sun, H.H., Yeda, K.T., Doench, J.G., et al. (2013). Discovery and characterization of super-enhancer-associated dependencies in diffuse large B cell lymphoma. Cancer Cell *24*, 777–790.

Dey, A., Chitsaz, F., Abbasi, A., Misteli, T., and Ozato, K. (2003). The double bromodomain protein Brd4 binds to acetylated chromatin during interphase and mitosis. Proc. Natl. Acad. Sci. USA *100*, 8758–8763.

Di Micco, R., Fontanals-Cirera, B., Low, V., Ntziachristos, P., Yuen, S.K., Lovell, C.D., Dolgalev, I., Yonekubo, Y., Zhang, G., Rusinova, E., et al. (2014). Control of embryonic stem cell identity by BRD4-dependent transcriptional elongation of super-enhancer-associated pluripotency genes. Cell Rep. *9*, 234–247.

Fierro-Fernández, M., Busnadiego, Ó., Sandoval, P., Espinosa-Díez, C., Blanco-Ruiz, E., Rodríguez, M., Pian, H., Ramos, R., López-Cabrera, M., García-Bermejo, M.L., and Lamas, S. (2015). miR-9-5p suppresses pro-fibrogenic transformation of fibroblasts and prevents organ fibrosis by targeting NOX4 and TGFBR2. EMBO Rep. *16*, 1358–1377.

Filippakopoulos, P., Qi, J., Picaud, S., Shen, Y., Smith, W.B., Fedorov, O., Morse, E.M., Keates, T., Hickman, T.T., Felletar, I., et al. (2010). Selective inhibition of BET bromodomains. Nature *468*, 1067–1073.

Filippakopoulos, P., Picaud, S., Mangos, M., Keates, T., Lambert, J.P., Barsyte-Lovejoy, D., Felletar, I., Volkmer, R., Müller, S., Pawson, T., et al. (2012). Histone recognition and large-scale structural analysis of the human bromodomain family. Cell *149*, 214–231.

Gillette, T.G., and Hill, J.A. (2015). Readers, writers, and erasers: chromatin as the whiteboard of heart disease. Circ. Res. *116*, 1245–1253.

Haldar, S.M., and McKinsey, T.A. (2014). BET-ting on chromatin-based therapeutics for heart failure. J. Mol. Cell. Cardiol. *74*, 98–102.

Hnisz, D., Abraham, B.J., Lee, T.I., Lau, A., Saint-André, V., Sigova, A.A., Hoke, H.A., and Young, R.A. (2013). Super-enhancers in the control of cell identity and disease. Cell *155*, 934–947.

Hnisz, D., Schuijers, J., Lin, C.Y., Weintraub, A.S., Abraham, B.J., Lee, T.I., Bradner, J.E., and Young, R.A. (2015). Convergence of developmental and oncogenic signaling pathways at transcriptional super-enhancers. Mol. Cell *58*, 362–370.

Jang, M.K., Mochizuki, K., Zhou, M., Jeong, H.S., Brady, J.N., and Ozato, K. (2005). The bromodomain protein Brd4 is a positive regulatory component of P-TEFb and stimulates RNA polymerase II-dependent transcription. Mol. Cell *19*, 523–534.

Kao, D.P., Lowes, B.D., Gilbert, E.M., Minobe, W., Epperson, L.E., Meyer, L.K., Ferguson, D.A., Volkman, A.K., Zolty, R., Borg, C.D., et al. (2015). Therapeutic molecular phenotype of β-blocker-associated reverse-remodeling in nonischemic dilated cardiomyopathy. Circ Cardiovasc Genet *8*, 270–283.

Korb, E., Herre, M., Zucker-Scharff, I., Darnell, R.B., and Allis, C.D. (2015). BET protein Brd4 activates transcription in neurons and BET inhibitor Jq1 blocks memory in mice. Nat. Neurosci. *18*, 1464–1473.

Langmead, B., and Salzberg, S.L. (2012). Fast gapped-read alignment with Bowtie 2. Nat. Methods *9*, 357–359.

Lovén, J., Hoke, H.A., Lin, C.Y., Lau, A., Orlando, D.A., Vakoc, C.R., Bradner, J.E., Lee, T.I., and Young, R.A. (2013). Selective inhibition of tumor oncogenes by disruption of super-enhancers. Cell *153*, 320–334.

Lowes, B.D., Gilbert, E.M., Abraham, W.T., Minobe, W.A., Larrabee, P., Ferguson, D., Wolfel, E.E., Lindenfeld, J., Tsvetkova, T., Robertson, A.D., et al. (2002). Myocardial gene expression in dilated cardiomyopathy treated with beta-blocking agents. N. Engl. J. Med. *346*, 1357–1365.

Mayer, S.C., Gilsbach, R., Preissl, S., Monroy Ordonez, E.B., Schnick, T., Beetz, N., Lother, A., Rommel, C., Ihle, H., Bugger, H., et al. (2015). Adrenergic repression of the epigenetic reader MeCP2 facilitates cardiac adaptation in chronic heart failure. Circ. Res. *117*, 622–633.

McKinsey, T.A. (2012). Therapeutic potential for HDAC inhibitors in the heart. Annu. Rev. Pharmacol. Toxicol. *52*, 303–319.

Meloche, J., Potus, F., Vaillancourt, M., Bourgeois, A., Johnson, I., Deschamps, L., Chabot, S., Ruffenach, G., Henry, S., Breuils-Bonnet, S., et al. (2015). Bromodomain-containing protein 4: the epigenetic origin of pulmonary arterial hypertension. Circ. Res. *117*, 525–535.

Olive, M., Krylov, D., Echlin, D.R., Gardner, K., Taparowsky, E., and Vinson, C. (1997). A dominant negative to activation protein-1 (AP1) that abolishes DNA binding and inhibits oncogenesis. J. Biol. Chem. *272*, 18586–18594.

Olson, E.N. (2014). MicroRNAs as therapeutic targets and biomarkers of cardiovascular disease. Sci. Transl. Med. *6*, 239ps3.

Pnueli, L., Rudnizky, S., Yosefzon, Y., and Melamed, P. (2015). RNA transcribed from a distal enhancer is required for activating the chromatin at the promoter of the gonadotropin α-subunit gene. Proc. Natl. Acad. Sci. USA *112*, 4369–4374.

Preissl, S., Schwaderer, M., Raulf, A., Hesse, M., Grüning, B.A., Köbele, C., Backofen, R., Fleischmann, B.K., Hein, L., and Gilsbach, R. (2015). Deciphering the epigenetic code of cardiac myocyte transcription. Circ. Res. *117*, 413–423.

Renaud, L., Harris, L.G., Mani, S.K., Kasiganesan, H., Chou, J.C., Baicu, C.F., Van Laer, A., Akerman, A.W., Stroud, R.E., Jones, J.A., et al. (2015). HDACs regulate miR-133a expression in pressure overload induced cardiac fibrosis. Circ Heart Fail *8*, 1094–1104.

Sano, M., and Schneider, M.D. (2004). Cyclin-dependent kinase-9: an RNAPII kinase at the nexus of cardiac growth and death cascades. Circ. Res. *95*, 867–876.

Sayed, D., He, M., Yang, Z., Lin, L., and Abdellatif, M. (2013). Transcriptional regulation patterns revealed by high resolution chromatin immunoprecipitation during cardiac hypertrophy. J. Biol. Chem. *288*, 2546–2558.

Shi, J., Wang, Y., Zeng, L., Wu, Y., Deng, J., Zhang, Q., Lin, Y., Li, J., Kang, T., Tao, M., et al. (2014). Disrupting the interaction of BRD4 with diacetylated Twist suppresses tumorigenesis in basal-like breast cancer. Cancer Cell *25*, 210–225.

Simpson, P.C., Long, C.S., Waspe, L.E., Henrich, C.J., and Ordahl, C.P. (1989). Transcription of early developmental isogenes in cardiac myocyte hypertrophy. J. Mol. Cell. Cardiol. *21* (*Suppl 5*), 79–89.

Spiltoir, J.I., Stratton, M.S., Cavasin, M.A., Demos-Davies, K., Reid, B.G., Qi, J., Bradner, J.E., and McKinsey, T.A. (2013). BET acetyl-lysine binding proteins control pathological cardiac hypertrophy. J. Mol. Cell. Cardiol. *63*, 175–179.

Stratton, M.S., and McKinsey, T.A. (2015). Acetyl-lysine erasers and readers in the control of pulmonary hypertension and right ventricular hypertrophy. Biochem. Cell Biol. *93*, 149–157.

Trapnell, C., Williams, B.A., Pertea, G., Mortazavi, A., Kwan, G., van Baren, M.J., Salzberg, S.L., Wold, B.J., and Pachter, L. (2010). Transcript assembly and quantification by RNA-Seq reveals unannotated transcripts and isoform switching during cell differentiation. Nat. Biotechnol. *28*, 511–515.

van Berlo, J.H., Maillet, M., and Molkentin, J.D. (2013). Signaling effectors underlying pathologic growth and remodeling of the heart. J. Clin. Invest. *123*, 37–45.

van Rooij, E., and Olson, E.N. (2012). MicroRNA therapeutics for cardiovascular disease: opportunities and obstacles. Nat. Rev. Drug Discov. *11*, 860–872.

Wang, K., Long, B., Zhou, J., and Li, P.F. (2010). miR-9 and NFATc3 regulate myocardin in cardiac hypertrophy. J. Biol. Chem. *285*, 11903–11912.

Weitzel, L.B., Ambardekar, A.V., Brieke, A., Cleveland, J.C., Serkova, N.J., Wischmeyer, P.E., and Lowes, B.D. (2013). Left ventricular assist device effects on metabolic substrates in the failing heart. PLoS ONE *8*, e60292.

Whyte, W.A., Orlando, D.A., Hnisz, D., Abraham, B.J., Lin, C.Y., Kagey, M.H., Rahl, P.B., Lee, T.I., and Young, R.A. (2013). Master transcription factors and mediator establish super-enhancers at key cell identity genes. Cell *153*, 307–319.

Wu, S.Y., Lee, A.Y., Lai, H.T., Zhang, H., and Chiang, C.M. (2013). Phospho switch triggers Brd4 chromatin binding and activator recruitment for gene-specific targeting. Mol. Cell *49*, 843–857.

Xie, M., and Hill, J.A. (2013). HDAC-dependent ventricular remodeling. Trends Cardiovasc. Med. *23*, 229–235.

Xing, W., Zhang, T.C., Cao, D., Wang, Z., Antos, C.L., Li, S., Wang, Y., Olson, E.N., and Wang, D.Z. (2006). Myocardin induces cardiomyocyte hypertrophy. Circ. Res. *98*, 1089–1097.

Yang, Z., Yik, J.H., Chen, R., He, N., Jang, M.K., Ozato, K., and Zhou, Q. (2005). Recruitment of P-TEFb for stimulation of transcriptional elongation by the bromodomain protein Brd4. Mol. Cell *19*, 535–545.

Yuva-Aydemir, Y., Simkin, A., Gascon, E., and Gao, F.B. (2011). MicroRNA-9: functional evolution of a conserved small regulatory RNA. RNA Biol. *8*, 557–564.

Zhang, Y., Liu, T., Meyer, C.A., Eeckhoute, J., Johnson, D.S., Bernstein, B.E., Nusbaum, C., Myers, R.M., Brown, M., Li, W., and Liu, X.S. (2008). Model-based analysis of ChIP-Seq (MACS). Genome Biol. *9*, R137.